

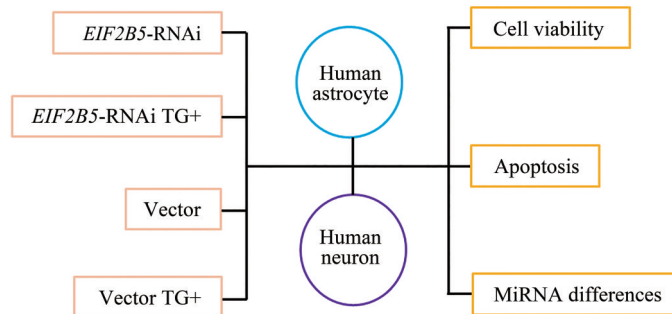
The Differing Fortunes and miRNA Clusters Between Human Astrocytes and Neurons After Endoplasmic Reticulum Stress With Downregulation of *EIF2B5**

CHEN Na^{1,2)}, WANG Jing-Min¹⁾, JIANG Yu-Wu¹⁾, WU Ye^{1)**}

¹⁾Department of Pediatrics, Peking University First Hospital, Beijing 100034, China;

²⁾Department of Pediatrics, Beijing Tiantan Hospital, Capital Medical University, Beijing 100070, China)

Graphical abstract



Abstract Objective Human astrocytes and human neurons were transfected with *EIF2B5*-RNAi vectors or blank as cell model to investigate the causes that white matter glial cells selectively involved in vanishing white matter disease. **Methods** Apoptosis and cell viability were measured in human astrocytes and neurons with *EIF2B5*-RNAi or blank vector before or after the stimulation of endoplasmic reticulum stress (ERS). The sequence of known and unknown microRNAs was performed to screen those participated in regulating the response of ERS. **Results** Under the baseline condition, apoptosis rates were detected higher in human astrocytes with *EIF2B5*-RNAi and cell viability decreased significantly than the wild-type and neurons. More pieces of miRNAs regulated the ERS rescue in astrocytes with blank vectors than the *EIF2B5*-RNAi group. In the cluster analysis, 5 pieces of miRNAs were identified as key components in pathway network. **Conclusion** The recovery of human astrocytes from ERS may be more dependent on the numerous miRNAs than neurons for cell proliferation and differentiation. The eroded clusters of miRNAs may promote spontaneous apoptosis and cell viability decrease in human astrocytes with *EIF2B5*-RNAi. As a result, it reduced the chance of survival in human astrocytes with *EIF2B5*-RNAi after ERS crisis.

Key words vanishing white matter disease, human astrocytes, human neurons, endoplasmic reticulum stress, apoptosis, miRNAs differences

DOI: 10.16476/j.pibb.2022.0449

Vanishing white matter disease (VWM) is an autosomal recessive leukodystrophy that develop all ages and life threatening at an early onset age. It is caused by mutations in any of the genes of *EIF2B1-5* encoding the 5 subunits of eukaryotic translation initiation factor 2B (eIF2B). *EIF2B1-5* are house-keeping genes and expressed ubiquitously, however,

VWM manifests as a leukoencephalopathy with

* This work was supported by grants from The National Natural Science Foundation of China (81171065, 30872793).

** Corresponding author.

Tel: 86-10-83572211, Email: dryewu@263.net

Received: September 19, 2022 Accepted: October 20, 2022

progressive cerebral white matter rarefaction and rapid neurological deterioration as the classical phenotype. VWM patients are sensitive to stress conditions as febrile infections, mild head trauma and acute fright, manifested as chronic progressive motor deterioration and relatively mild mental decline^[1-2]. Pathological findings from VWM patients include thin myelin sheaths and gelatinous, scarce white matter in the focal zone but the grey matter is generally spared or greatly preserved^[2-7]. On macroscopic examination showed foamy oligodendrocytes, meager astrogliosis with dysmorphic astrocytes and loss of oligodendrocytes by apoptosis. Mutations impair the activity of eIF2B and its function to couple protein synthesis to the cellular demands, leading to sustained activation of the unfolded protein response (UPR), especially during stress conditions^[6,8]. In our previous study, eIF2B mutant oligodendrocytes are susceptible to endoplasmic reticulum stress (ERS) stimulation. The UPR pathway is activated under basic condition and overactivated after ERS, with the depression of autophagy, resulting to the inability to terminate ERS and a large amount of apoptotic death in oligodendrocytes^[9-10]. MicroRNAs (miRNA) play important parts in cell proliferation and differentiation for promoting cell survival. Several chemicals have been identified work through miRNAs^[11-13]. However, up to now limited studies on the miRNAs in the pathogenesis of VWM^[11-13]. Astrocytes are essential in central nervous system (CNS) for the paucity of astrogliosis and abnormal morphology of astrocytes in VWM patient leading to the vanished white matter^[2]. In this study, human astrocytes and human neurons were transfected with *EIF2B5*-RNAi or blank vector for comparison under basic condition or after ERS. To get a better understanding of the reasons that glial selectively involved in VWM, different destinies were measured between neurons and astrocytes with *EIF2B5* knockdown after ERS stimulation and the clusters of upstream miRNAs were also detected.

1 Materials and methods

1.1 Culture of primary human astrocytes and neurons

Primary human astrocytes (Catalog# 1800) (HA) and primary human neurons (Catalog# 1520-10), and the culture medium for human astrocytes (Catalog#

1801) and human neurons (Catalog# 1521) were purchased from ScienCell Research Laboratories, America. Cell culture and passage were the same as those of normal adherent cell culture. First the cell culture plates were covered with 0.1 g/L polylysine (PLL) (Sigma), 37° C 30 min, washing the culture plate twice with sterile ddH₂O, removing the residual liquid thoroughly, plating with cells for spare, changing medium after cell adhering to the plates after 16–18 h.

1.2 Vectors of *EIF2B5*-RNAi and lentiviral transduction

1.2.1 Vectors of *EIF2B5*-RNAi

The *EIF2B5* lentiviral vector sequence (NM_003907) was referred from the overexpression of *EIF2B5*-targeted RNAi (pBSU6-581i), published by Jörg Dietrich for human glial precursor cells (hGPC)^[5]. The carrier is pGLV2-U6-Puro constructed by Shanghai GenePharma Co., Ltd. The *EIF2B5* mRNA was degraded when the vector of pGLV2-U6 581i RNAi transfected in cells, called *EIF2B5* silence. The *EIF2B5*-targeted RNAi (pBSU6-581i) is as follows. *EIF2B5* hs581i forward: 5'-GATCCCCCTCGTTGCCACGAAGACAATTCAAGAGATTGTCTTCGTGGCAACGAGTTTTTGGAAA-3'; *EIF2B5* hs581i reverse: 5'-AGCTTTTCCAAAACTCGTTGCCACGAAGACAATCTCTTGAATTGTCTTCGTGGCAACGAGGG-3'.

1.2.2 Transduction efficiency of *EIF2B5*-RNAi

Transfection efficiency was validated with real-time PCR for *EIF2B5* transcription and Western blot for FLAG-tag. The vectors with *EIF2B5*-RNAi or blank were transfected into human astrocytes with an optimized condition. 72 h after transfection, the cells were harvested for the following studies. The forward primer of *EIF2B5*: 5'-TGGAGTGGAGGTTTCGATATGAT-3'; the reverse primer: 5'-GGTTCCCTAGGATCTCCTCAT-3'.

1.3 miRNA sequencing

Eight groups of lentiviral vectors were transferred human astrocytes or human neurons respectively. The miRNAs were compared pairwise before and after ERS. 1 μmol/L Thapsigargin (TG, #T9033, Sigma-Aldrich, USA) was used for the stimulation of ERS. According to the screening strategy, differences greater than 2 times were considered significant. The marks T01 to T04 represent human astrocytes (T01 and T02 with TG,

T03 and T04 without TG); T05–T08 are neuron groups (T05 and T07 are TG group, T06 and T08 without TG). Vector (v) representing blank vector and *EIF2B5*-RNAi (i) represents *EIF2B5*-RNAi groups for neuron or astrocyte. The marks include T01 (Astrocyte vTG), T02 (Astrocyte iTG), T03 (Astrocyte i), T04 (Astrocyte v), T05 (Neuron iTG), T06 (Neuron i), T07 (Neuron vTG) and T08 (Neuron v).

High-throughput was performed by illumina HiSeq/MiSeq (Beijing Berry Genomics Co., Ltd). The original image data files obtained from illumine sequencing was analyzed by Base Calling and transferred to Sequenced Reads (raw reads). They were documented as the file format of FASTQ (fq), which includes reads and sequencing quality information. The primary analysis of raw data was completed by the procedure of de-coupling, de-low quality, de-contamination and statistical sequence length distribution. Clean reads obtained from primary analysis were compared with the ncRNA library, which were classified and annotated, removing rRNA, tRNA, snRNA, snoRNA. The reads were then aligned to the reference genome and miRNA base, calculating miRNA expression, annotating the known miRNAs and predicting new miRNAs for further analysis.

The length of clean reads distribution: the number of 18–31 nt clean reads and respective percentage of total were calculated, plotting the length distribution of reads. Generally, the length of small RNA ranges 18–31 nt, and the peak of distribution helps us to judge the type of small RNAs. For example, miRNA was concentrated at 21 or 22 nt, siRNA at 24 nt and piRNA at 30 nt. The Venn diagram method was used to visually display the differences in the number of known miRNAs, predicting new miRNAs in multiple samples, also with RFAM alignment, base bias analysis and clean reads after removing rRNA, scRNA, snRNA, snoRNA, tRNA and ncRNA compared from the reference genome. The total matched reads were compared with the corresponding genome to predict the known miRNA target genes.

1.4 Detection of cell apoptosis and viability for the tolerance of ERS

Rates of apoptosis and cell viability were measured by Annexin V-FITC and quantitated by flow

cytometry (FCM). FCM detects the rates of cell apoptosis under basic condition or after ERS stimulation. Astrocytes or neurons were double-labeled with Annexin V-FITC/propidium iodide (PI) by apoptosis detection kit (#KGA108, KeyGEN BioTECH, Beijing, China). Normally, the phosphatidylserine (PS) is only distributed in the inner side of the lipid bilayer of the cell membrane, in the early stage of apoptosis however, PS turns from the inner side of the lipid membrane to the outside. Annexin V has a high affinity for phosphatidyl serine, so it could bind to the membrane of early apoptotic cells through the PS exposed on the outside of the cell. PI is a nuclei acid dye which could not pass through the intact cell membrane but the late apoptotic cells and dead cells could be dyed red. Therefore the use of Annexin V and PI helps to distinguish cells in different status of apoptosis from dead cells, as apoptotic cells (Annexin V+, PI-), necrotic cells (Annexin V+, PI+), no apoptotic or necrotic cells (Annexin V-, PI-). Astrocytes or neurons without transfection were set as baseline (0 h), comparing with the *EIF2B5*-RNAi or blank vector transfected cells. Cell viability was measured under basic condition and at different time points of 8 h, 24 h and 48 h after ERS stimulation with the Cell Counting Kit-8 (CCK-8) (#CK04, Dojindo Molecular Technologies, Japan). Statistical differences between two groups were determined by two-tailed unpaired *t*-test. One-way analysis of variance was for more than two groups. $P < 0.05$ was considered significantly different (* $P < 0.05$, ** $P < 0.01$, *** $P < 0.001$). The results were repeated 3 times separately.

2 Results

2.1 The primary human astrocytes with *EIF2B5* knockdown showed increased apoptosis rates and decreased cell viability under basic condition and further reduced the cell survival after ERS stimulation

Primary human astrocytes transfected with PGLV2-U6 581i RNA interference vector of *EIF2B5* were compared with astrocytes with PGLV2-U6 control vector. The changes of cell viability and apoptosis level were observed at basal state (natural culture) and ERS stimulation (1 $\mu\text{mol/L}$ TG). In basal state, human astrocytes without transfection and transfected with control vector began to proliferate at

48–72 h with the extension of culture time, and the cell viability increased. However, the viability of astrocytes with *EIF2B5* knockdown began to decline at 8 h of natural culture, and remained at a low level at 24, 48 and 72 h (Figure 1a). Astrocytes without transfection or ERS stimulation (TG⁻) were modulated as the baseline of apoptosis. FCM results showed that the apoptosis level of primary human astrocytes transfected with *EIF2B5* PGLV2-U6 581i RNA interference vector was significantly higher than that of PGLV2-U6 control vector group after 48 h of

natural culture (Figure 1c).

After ERS stimulation, the viability of astrocytes decreased to some extent in the non-transfected group, the control vector transfected group and the *EIF2B5* knockdown group. The cell viability decreased rapidly in the *EIF2B5* knockdown group at 8–24 h after ERS stimulation, and remained at a low level at 48–72 h after ERS stimulation (Figure 1b). The apoptotic rates of *EIF2B5* knockdown group were significantly higher than control vector group after ERS induction (Figure 1c).

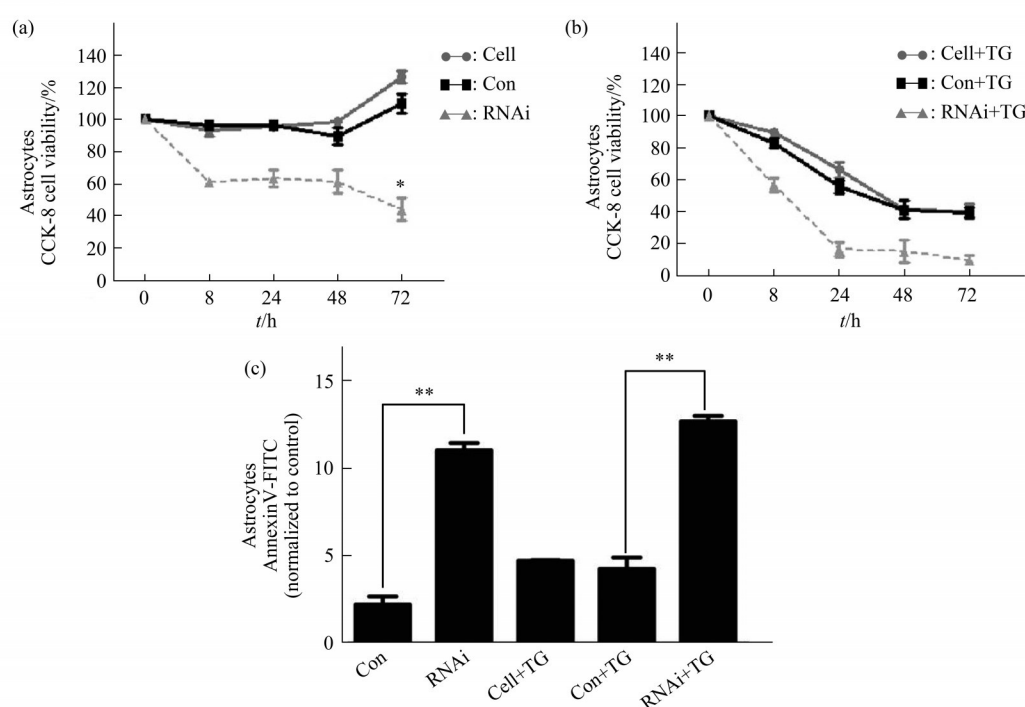


Fig. 1 Detection of viability and apoptosis rate in primary human astrocytes under basal condition and after ERS

(a) Comparison of cell viability levels under basic condition (natural culture), not transfected cells (Con) and *EIF2B5* knockdown cells. (b) Cell viability comparison between groups after ERS (1 $\mu\text{mol/L}$ TG). (c) Comparison of apoptosis levels under basal state and ERS stimulation for 48 h in different groups. Statistical differences between *EIF2B5*-RNAi and blank vector groups were determined by two-tailed unpaired *t*-test. * $P < 0.05$, ** $P < 0.01$.

2.2 Human neurons with *EIF2B5* knockdown did not show increased apoptosis and decreased viability with culture time in the basal condition

Cell viability is not reduced in neurons transfected with *EIF2B5* pGLV2-U6 581i RNA or pGLV2-U6 blank vector groups in basal condition (Figure 2a). FCM analysis showed that there was no significant difference in apoptosis level between *EIF2B5* knockdown group and control vector group after 48 h of natural culture (Figure 2c).

After 8 h of ERS stimulation, the cell viability of *EIF2B5* knockdown group, control vector group and not transfected group decreased rapidly compared with the basal state. There was no significant difference in cell viability between the *EIF2B5* knockdown group and the control vector group, or between the control vector group and the group without transfection (Figure 2b). FCM showed that *EIF2B5* knockdown neurons showed a significant increase in apoptosis after ERS stimulation (Figure 2c).

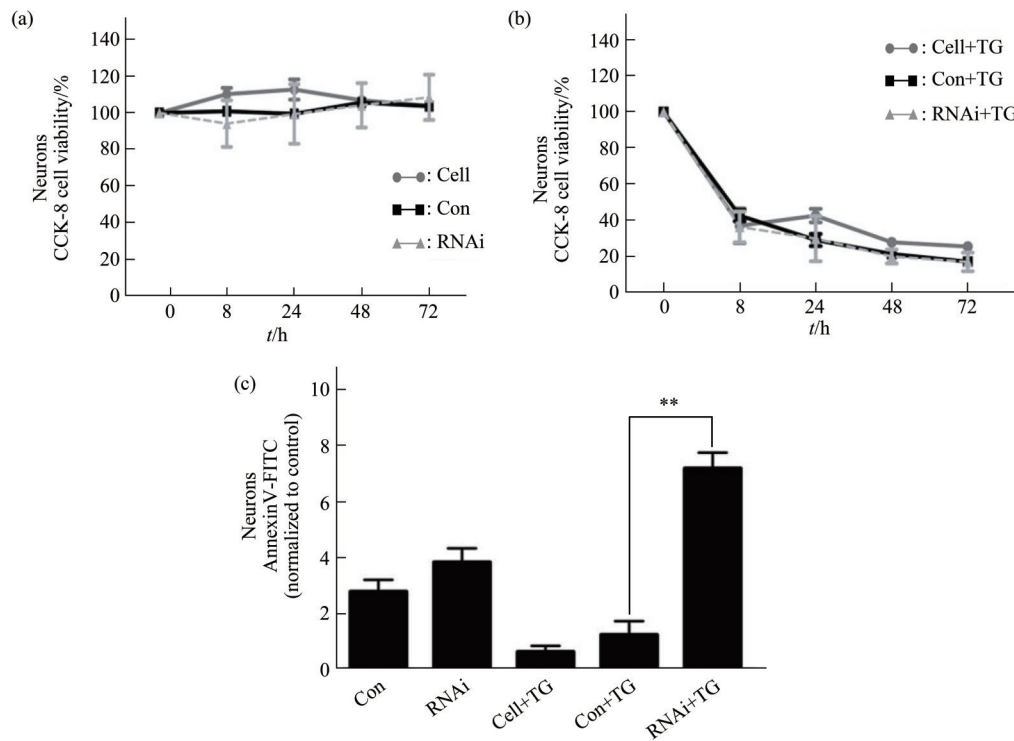


Fig. 2 Cell viability and apoptosis level of human neurons under basic condition and after ERS

(a) Comparison of cell viability of not transfected cells (Cell), transfected empty vector (Con) and *EIF2B5* knockdown (RNAi) cell groups in basal state (natural culture without TG). (b) Cell viability is declining in all groups after ERS (1 $\mu\text{mol/L}$ TG). (c) Apoptosis rates comparison before and 48 h after ERS stimulation. Statistical differences between *EIF2B5*-RNAi and blank vector groups were determined by two-tailed unpaired *t*-test. ** $P < 0.01$.

2.3 Astrocytes require more miRNAs to participate in regulation than neurons in the basal condition and the number of miRNAs involved in regulation decreased significantly after *EIF2B5*-RNAi

More pieces of known and unknown miRNAs were measured participated in the regulation after ERS stimulation in human astrocytes, but the number of miRNAs involved reduced after the transfection of *EIF2B5*-RNAi vectors. Among the known miRNA data, there were 345 differentially expressed miRNAs between wild-type and *EIF2B5*-RNAi transfected human astrocytes in the basal state.

It was detected 350 miRNAs in wild-type human astrocytes after ERS stimulation, while only 5 differential miRNAs in *EIF2B5*-RNAi human astrocytes. In human neurons, there were 43 different miRNAs between wild-type and *EIF2B5*-knock down

human neurons in the basal state. After ERS stimulation, 46 differentially expressed miRNAs were obtained in wild-type human neurons and human neurons with *EIF2B5*-knock detected 15 differentially expressed miRNAs.

The miRNAs that engaged in the regulation after ERS crisis were screening in astrocytes and neurons transfected with *EIF2B5*-RNAi (Figure 3a). N1, the miRNA difference present in wild-type and *EIF2B5*-RNAi astrocytes; N2, miRNA changes after ERS stimulation in wild-type astrocytes; N3, miRNAs involved in ERS regulation of *EIF2B5*-RNAi transfected astrocytes; N2 was compared with N3 to obtain N4, and then the differences between wild-type and RNAi human astrocytes before ERS stimulation were compared to obtain N9 (miRNAs differences in astrocytes with or without *EIF2B5*-RNAi transfection before and after ERS). Parallel experiments to

compare human neurons: N5 is the miRNAs difference between wild-type and *EIF2B5*-RNAi human neurons. N6 and N7 respectively represent the difference in miRNA expression between wild-type and *EIF2B5*-RNAi human neurons after ERS stimulation. After N8, N10 was obtained by comparing the difference between wild-type and *EIF2B5*-RNAi human neurons before ERS stimulation (miRNA differences in human neurons with wild type or *EIF2B5*-RNAi vectors after ERS). N9 and N10 were compared to determine which miRNAs were significantly changed in N11, which is the final miRNA changes in the wild-type and *EIF2B5*-RNAi human astrocytes and human neurons after ERS stimulation. Then go back to the original database and find out which procedure the changes came from (Figure 3b).

The results of N11 screened above were substituted in to find common and unique miRNAs among the different samples (Figure 3b). Finding out the natural differences in astrocytes and neurons, N12 was harvested. Comparing the miRNA differences between wild-type astrocytes and neurons, finding out the same miRNAs we obtained in N11, getting 58

pieces of miRNA as N12 for background data. N13 was obtained after screening out the miRNAs differences between human astrocytes and human neurons transfected with *EIF2B5*-RNAi, finding out the same miRNAs in N11. N13 is derived from the miRNA differences between human astrocytes and human neurons caused by *EIF2B5*-RNAi factor, and the number of 190 pieces of miRNA as N14 is obtained by subtracting the natural difference between the two types of cells. Identifying the different pieces of miRNA expression between human astrocytes and neurons with *EIF2B5*-RNAi after ERS stimulation, and then to find the same miRNA in N11, getting N15, removing the N12 part, obtaining the number of 196 pieces of miRNAs as N16.

The selected miRNAs were subjected to signal pathway cluster analysis and finally 5 known miRNAs, hsa-miR-335-5p, hsa-miR-92a-3p, hsa-miR-548aj-5p, hsa-miR-548g-5p, hsa-miR-548x-5p, were emerged from the miRNA data pool, which play key roles in the connection of multiple signal pathways, participating in cell proliferation and differentiation (Figure 4).

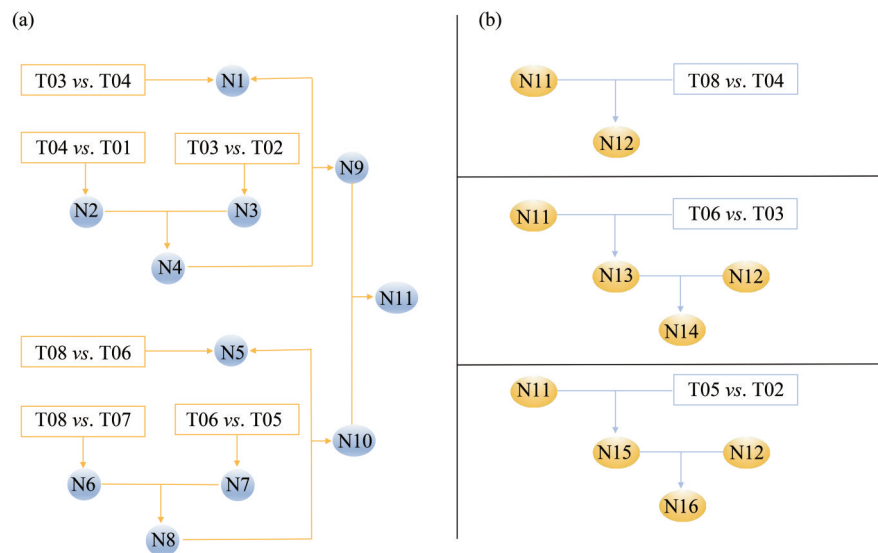


Fig. 3 The miRNA comparison strategies of astrocytes and neurons in basal state and after ERS in different groups

The number of T01 represents human astrocytes transfected with control blank vector and TG added group; T02, astrocytes (*EIF2B5*-RNAi transfected, TG+); T03, astrocytes (*EIF2B5*-RNAi transfected, TG-); T04, astrocytes (blank vector transfected, TG-); T05, human neurons (*EIF2B5*-RNAi transfected, TG+); T06, human neurons (*EIF2B5*-RNAi transfected, TG-); T07, human neurons (control blank vector transfected, TG+); T08, human neurons (blank vector transfected, TG-).

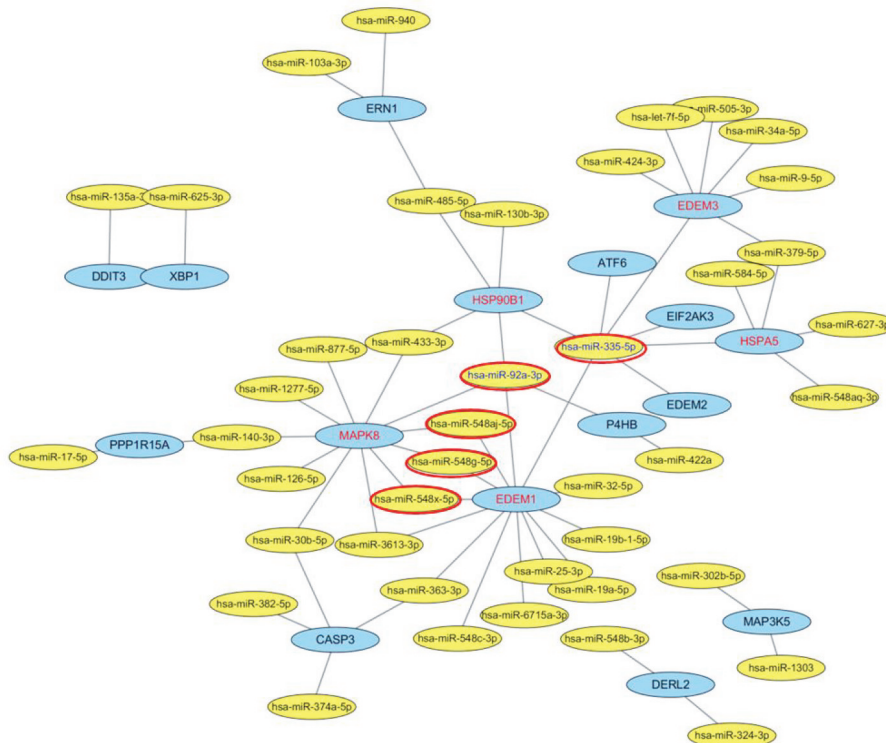


Fig. 4 The difference of miRNA expression was obtained between human astrocytes and human neurons transfected with *EIF2B5*-RNAi after ERS stimulation by screening strategy

The 5 known miRNAs were found to be key components of cell proliferation and differentiation by cluster analysis of miRNA signaling pathways.

3 Discussion

The eIF2B subunit has guanine nucleotide exchange factor (GEF) activity. It is a key component for protein translation initiation. It is still unknown why the white matter selectively involved in VWM patients, while the neurons in the brain is spared. Motor regression is more serious and earlier than intellectual damage in VWM patients. In our previous study on mutant oligodendrocytes, the UPR pathway was overactivated after ERS, and autophagy pathway clearing unfolded proteins was damaged, leading to massive apoptotic cell death^[10]. Astrocytes constitute the main part of the white matter of the brain and play an essential role in nutritional support and signal transmission for oligodendrocytes. The eIF2B subunit encoded by *EIF2B5*, is the largest one and the main functional domain of GEF catalysis^[14-15]. Studies in zebrafish have shown that mutation in *EIF2B5* may aggravate the response to stress and impair motor behavior with the effects on myelination, loss of oligodendrocyte precursor cells, increased apoptosis

in the CNS in a zebrafish with *EIF2B* mutants^[16].

The leukodystrophy may be due to defects in protein translation, as eIF2B is the important protein translation initiation factor. MiRNAs are non-coding RNAs with a length of 21–22 nt involved in post-transcriptional regulation of gene expression. *In vivo* evidence showed miRNA overexpressing in mice improved myelin thickness, and may enhance both oligodendrocyte differentiation and myelin synthesis^[17-18]. MiRNAs also participate in the pathogenesis of neurodegenerative disease by regulating astrocyte function through different mechanisms and may be potential treatment targets^[19]. MiRNAs also play an important role in regulating a large number of developmental processes and diseases through biological networks^[20-21].

As miRNAs are potent regulators and have been shown to drive multiple pathways, the impact of miRNA-miRNA interactions could be profound. Strategies designed for new individual miRNAs have limited effects, and most of them act in clusters, not many miRNA studies have considered the wider impact of miRNA on overall miRNA expression^[22].

MiRNAs may exert function in groups. Sequence and functional analysis *in vitro* for selecting the single piece of miRNA may not exhibit the whole pictures of its influence and individual miRNAs have limited effects. In our study, changes in the participating number of miRNAs were calculated. After detecting all known or unknown miRNAs with two-fold or more expression differences, it was found that more miRNAs were involved in the regulation of wild-type astrocytes after ERS stimulation, while fewer involved in the regulation of wild-type neurons after ERS stimulation. Astrocytes may be more dependent on miRNA regulation than neurons. However, when *EIF2B5* gene was knocked down in astrocytes, the number of miRNAs involved in the regulation after ERS stimulation was significantly reduced, accompanied with increased cell apoptosis and decreased cell viability. A series of comparison strategies were designed for screening which miRNA participated after ERS. The changes of miRNAs in wild-type or *EIF2B5* knockdown neurons and astrocytes with or without ERS stimulation were compared. The database was then returned to look for changes originating from natural differences, loss of function in *EIF2B5*, or ERS stimulation resulting in differences. Cluster analysis was performed on the final miRNAs with differences to find those closely related to each known pathway. Five potential meaningful known miRNAs were obtained. These 5 miRNAs serve as junctions that connecting different pathways which involved in many biological processes as cell proliferation, differentiation, apoptosis, and maturation through gene repression.

4 Conclusion

Astrocytes and oligodendrocytes, both of which belong to the secretory pathway, may rely more on numerous miRNAs for the regulation of repairment to promote survival after ERS compared with neurons. *EIF2B5*-RNAi human astrocytes have a serious shortage of miRNAs participated after ERS due to the spontaneous apoptosis, which may lead to failure to survive in the last stage. Endogenous non-coding RNAs as miRNAs participate in cell proliferation, differentiation and maturation. Further studies on related miRNAs provide diagnostic, prognostic markers and chemotherapeutic targets in VWM. The calculation of participated miRNAs and selected

miRNAs interference may serve as another observation marker besides cell apoptosis and vitality for the intervene of UPR pathway.

References

- [1] van der Knaap M S, Pronk J C, Scheper G C. Vanishing white matter disease. *Lancet Neurol*, 2006, **5**(5):413-423
- [2] Bugiani M, Boor I, Powers J M, *et al*. Leukoencephalopathy with vanishing white matter: a review. *J Neuropathol Exp Neurol*, 2010, **69**(10):987-996
- [3] van der Knaap M S, Barth P G, Gabreels F J, *et al*. A new leukoencephalopathy with vanishing white matter. *Neurology*, 1997, **48**(4):845-855
- [4] Rodriguez D, Gelot A, Della G B, *et al*. Increased density of oligodendrocytes in childhood ataxia with diffuse central hypomyelination (CACH) syndrome: neuropathological and biochemical study of two cases. *Acta Neuropathol*, 1999, **97**(5): 469-480
- [5] Dietrich J, Lacagnina M, Gass D, *et al*. *EIF2B5* mutations compromise GFAP+ astrocyte generation in vanishing white matter leukodystrophy. *Nat Med*, 2005, **11**(3):277-283
- [6] Ashrafi M R, Amanat M, Garshasbi M, *et al*. An update on clinical, pathological, diagnostic, and therapeutic perspectives of childhood leukodystrophies. *Expert Rev Neurother*, 2020, **20**(1): 65-84
- [7] Bugiani M, Postma N, Polder E, *et al*. Hyaluronan accumulation and arrested oligodendrocyte progenitor maturation in vanishing white matter disease. *Brain*, 2013, **136**(Pt 1):209-222
- [8] 陈娜, 代丽芳, 姜玉武, 等. 内质网应激后未折叠蛋白反应在神经退行性疾病发病机制中的作用. *生物化学与生物物理进展*, 2012, **39**(8):764-770
Chen N, Dai L, Jiang Y, *et al*. *Prog Biochem Biophys*, 2012, **39**(8): 764-770
- [9] 陈娜, 代丽芳, 吴晔等. 未折叠蛋白反应通路持续过度激活在白质消融性白质脑病发病中的作用. *中华实用儿科临床杂志*, 2015, **30**(12):895-899
Chen N, Dai L, Wu Y, *et al*. *Chin J Appl Clin Pediatr*, 2015, **30**(12): 895-899
- [10] Chen N, Dai L, Jiang Y, *et al*. Endoplasmic reticulum stress intolerance in *EIF2B3* mutant oligodendrocytes is modulated by depressed autophagy. *Brain Dev*, 2016, **38**(5):507-515
- [11] Motawi T K, Al-Kady R H, Abdelraouf S M, *et al*. Empagliflozin alleviates endoplasmic reticulum stress and augments autophagy in rotenone-induced Parkinson's disease in rats: targeting the GRP78/PERK/eIF2alpha/CHOP pathway and miR-211-5p. *Chem Biol Interact*, 2022, **362**:110002
- [12] Chatterjee N, Fraile-Bethencourt E, Baris A, *et al*. MicroRNA-494 regulates endoplasmic reticulum stress in endothelial cells. *Front Cell Dev Biol*, 2021, **9**:671461
- [13] Jang J H, Lee T J. The role of microRNAs in cell death pathways. *Yeungnam Univ J Med*, 2021, **38**(2):107-117

- [14] Bugiani M, Vuong C, Breur M, *et al.* Vanishing white matter: a leukodystrophy due to astrocytic dysfunction. *Brain Pathol*, 2018, **28**(3):408-421
- [15] Fogli A, Schiffmann R, Bertini E, *et al.* The effect of genotype on the natural history of eIF2B-related leukodystrophies. *Neurology*, 2004, **62**(9):1509-1517
- [16] Keefe M D, Soderholm H E, Shih H Y, *et al.* Vanishing white matter disease expression of truncated *EIF2B5* activates induced stress response. *Elife*, 2020, **9**: e56319
- [17] Lin S T, Huang Y, Zhang L, *et al.* MicroRNA-23a promotes myelination in the central nervous system. *Proc Natl Acad Sci USA*, 2013, **110**(43):17468-17473
- [18] Shin V Y, Chu K M. MiRNA as potential biomarkers and therapeutic targets for gastric cancer. *World J Gastroenterol*, 2014, **20**(30):10432-10439
- [19] Bai Y, Su X, Piao L, *et al.* Involvement of astrocytes and microRNA dysregulation in neurodegenerative diseases: from pathogenesis to therapeutic potential. *Front Mol Neurosci*, 2021, **14**:556215
- [20] Pidikova P, Reis R, Herichova I. miRNA clusters with down-regulated expression in human colorectal cancer and their regulation. *Int J Mol Sci*, 2020, **21**(13):4633
- [21] Yi R, Fuchs E. MicroRNAs and their roles in mammalian stem cells. *J Cell Sci*, 2011, **124**(Pt 11):1775-1783
- [22] Hill M, Tran N. miRNA interplay: mechanisms and consequences in cancer. *Dis Model Mech*, 2021, **14**(4): dmm047662

*EIF2B5*表达下调的人星形胶质细胞与人神经元 在内质网应激后细胞存活及miRNA表达的差异*

陈娜^{1,2)} 王静敏¹⁾ 姜玉武¹⁾ 吴晔^{1)**}

(¹⁾ 北京大学第一医院儿科, 北京 100034;

(²⁾ 首都医科大学附属北京天坛医院儿科, 北京 100070)

摘要 **目的** 探讨白质消融性白质脑病中胶质细胞选择性受累而神经元受累轻微的原因。**方法** 将*EIF2B5*-RNAi表达载体转染至人星形胶质细胞和人神经元, 检测基础状态下及内质网应激(endoplasmic reticulum stress, ERS)后细胞凋亡和活力, 检测参与ERS调控的已知和未知miRNA, 筛选*EIF2B5*-RNAi人星形胶质细胞在ERS后miRNA变化。**结果** 与*EIF2B5*-RNAi人神经元相比, 星形胶质细胞自发凋亡及细胞活力下降。较之神经元, 更多miRNA参与星形胶质细胞ERS刺激后的调控, *EIF2B5*-RNAi组参与调控的miRNA数目显著减少。聚类分析发现, 5条已知miRNA是通路连接的关键组分。**结论** 人星形胶质细胞在ERS后可能更加依赖众多促细胞增殖分化的miRNA修复, 而*EIF2B5*-RNAi人星形胶质细胞存在自发凋亡, ERS后严重减少的miRNA可能导致细胞无法存活。

关键词 白质消融性白质脑病, 人星形胶质细胞, 人神经元, 内质网应激, 凋亡, miRNA表达差异

中图分类号 R72

DOI: 10.16476/j.pibb.2022.0449

* 国家自然科学基金(81171065, 30872793)资助项目。

** 通讯联系人。

Tel: 010-83573238, E-mail: dryewu@263.net

收稿日期: 2022-09-19, 接受日期: 2022-10-20